Enthalpies of formation and crystallization of amorphous $Zr_{1-x}Al_x$ and $Zr_{1-x}Ni_x$ alloys: calculations compared with measurements*

E. Ma and M. Atzmon

Department of Nuclear Engineering, University of Michigan, Ann Arbor, MI 48109-2104 (USA)

Abstract

The enthalpies of formation of amorphous $Zr_{1-x}Al_x$ and $Zr_{1-x}Ni_x$ alloys have been calculated based on CALPHAD data and compared with experimentally determined values. A direct extrapolation of the thermodynamic functions of the undercooled liquid significantly underestimates the stability of the amorphous phase. When including the effects of the excess specific heat of the undercooled liquid, ΔC_p, good quantitative agreement between the calculations and experimental data has been achieved, in particular for the Zr–Ni case. Using the same ΔC_p functions, the enthalpy of crystallization of the amorphous alloys in both systems has been computed and found to agree well with the same quantity directly obtained from calorimetric measurements. These calculated enthalpy of crystallization data have also been employed in an alternative approach to calculating the enthalpy of formation of the amorphous alloys; such calculations are in excellent agreement with experimental values in both Zr–Al and Zr–Ni cases. It is shown that the enthalpy–composition diagram measured or calculated using our approaches can be used as a good approximation to the free energy–composition diagram in predicting the homogeneity range of the amorphous phase for low synthesis temperatures.

1. Introduction

Amorphous metallic alloys are useful for a variety of applications due to their superior properties compared with their crystalline counterparts. The metastability of an amorphous structure, however, requires that certain thermodynamic and kinetic conditions be met for its formation and stabilization [1]. It has been suggested [1, 2] that, provided that kinetic constraints are imposed to avoid the formation of the more stable equilibrium compounds in the system, the free energy of the amorphous phase relative to competing crystalline phases determines the homogeneity range of the amorphous phase. Information regarding metastable phase equilibria involving an amorphous phase is therefore valuable. A thermodynamic characterization of a binary system has been shown to be essential in order to understand the formation and stability of the amorphous phase [2].

Most known amorphous metallic alloy phases are characterized by a negative heat of formation from the constituent elements. Moreover, for amorphous alloys formed by interdiffusion of elemental materials, a large

negative heat of mixing of the binary alloy provides the driving force for amorphization [1]. Measured data for the enthalpy of formation of amorphous alloys are available for a limited number of binary systems. A calculated heat of mixing table has been compiled by Miedema et al. for binary alloy combinations using a semi-empirical model [3]. Although the Miedema model has been applied with considerable success to predict amorphous phase formation and the stability range [4], it frequently encounters discrepancies when compared quantitatively with experimental data. This is also true for the two systems Zr–Al and Zr–Ni we investigate in this paper. For the equiatomic compounds, the Miedema model predicts heats of formation of -83 kJ mol^{-1} and -72 kJ mol^{-1} for ZrAl and ZrNi, respectively, whereas the measured values are -45 kJ mol^{-1} [5] and -50 kJ mol^{-1} [6(a), 6(b)], respectively. In fact, Miedema's tabulated enthalpy of mixing for a random amorphous alloy, without taking into account chemical ordering, known to be substantial in easy glass-forming systems [7], already reaches -44 kJ mol^{-1} and -49 kJ mol^{-1} for Zr–Al and Zr–Ni, respectively. Therefore, caution should be exercised when using values given by the Miedema model. Such discrepancies between model predictions and measurements have been noted before, e.g. in refs. 6(a) and 6(b).

Another common approach of thermodynamic evaluation of a binary system is the CALPHAD method [8], which uses analytical expressions to describe the free energy of various phases in a binary system. These expressions are derived from models, with parameters obtained from numerical fits to measured equilibrium data. Extrapolations are then used to predict metastable equilibria, with an undercooled liquid representing the amorphous phase. In these models, the free energy expression is usually a polynomial of first order in temperature, and its temperature-independent part is the enthalpy term. The CALPHAD method is usually preferred to the Miedema model since the former is based on more explicit thermodynamic data such as the equilibrium phase diagram. Nevertheless, CALPHAD calculations are sometimes also inadequate due to problems associated with insufficient experimental input, fitting errors, and invalid extrapolation to large undercooling [9]. The extrapolation error originates from insufficient knowledge of the temperature dependence of the thermodynamic properties. Although the heat capacities of an elemental liquid and its corresponding crystalline phase are very close to each other at the melting point and do not differ much in the undercooled regime, a substantial heat capacity difference has been observed for alloys [10(a), 10(b)]. It has been suggested that for a glass-forming liquid, its degree of order increases with undercooling until it freezes into a glass at the glass transition temperature. This results in a substantial excess specific heat of the undercooled liquid, ΔC_p, such that the enthalpy of the liquid becomes more negative with decreasing temperature.

Considerable work has been devoted to developing analytical approximations of the free energy (or enthalpy) change upon crystallization of an amorphous phase, since these quantities are important parameters affecting the thermodynamic prediction of glass formation as well as of nucleation of crystalline phases. Approximate formulae have been derived to calculate the enthalpy and free energy difference between undercooled liquids and crystalline solids [11–16]. These approximations vary somewhat mainly due to different choices of the excess specific heat of the liquid, which is unknown for most alloys. In order to calculate the enthalpy of crystallization for a binary alloy, assumptions have to be made on both the temperature and composition dependence of ΔC_p.

This paper presents thermodynamic characterization, i.e. calculations and measurements, of two binary systems, Zr–Al and Zr–Ni. We will mainly discuss the enthalpy of formation (ΔH_f) in this paper, because it is the quantity measured in calorimetry experiments. At low temperatures, entropy effects will not be large and the enthalpy of formation vs. composition diagram

should give a good approximation of the free energy vs. composition diagram [2]. This approximation will be discussed further at the end of this paper. Amorphous $Zr_{1-x}Al_x$ alloys have been formed only by mechanical alloying of elemental Zr and Al powders [17–19]. Amorphous Zr–Ni alloys on the other hand, have been formed by a variety of techniques [6(a), 20–25]. In Section 2 we first discuss the experimental enthalpy of crystallization data for amorphous $Zr_{1-x}Al_x$ and $Zr_{1-x}Ni_x$ alloys, determined from calorimetric measurements, and convert them into enthalpy of formation data using the known enthalpy of formation for equilibrium compounds [6]. In Section 3 we then compare the data described in Section 2 with CALPHAD data. We will not use the Miedema model in later discussions since we are attempting a quantitative match between model calculations and experimental data. In order to overcome the inaccuracies of the CALPHAD extrapolation so as to improve the agreement between the calculations and the experimental data, an effort is made in Section 4 to modify the CALPHAD method by incorporating an excess specific heat term for the undercooled liquid with assumed temperature dependence of ΔC_p. In Section 5 the enthalpy of crystallization is also computed with the same assumed ΔC_p functions, and compared with the very same quantity directly obtained from calorimetric measurements. The calculations of the enthalpy of crystallization also enable us to calculate the formation enthalpy of the amorphous phases in an alternative approach by making use of the enthalpy of formation data for equilibrium compounds. A comparison is made between the formation enthalpy calculations presented in Sections 4 and 5. We also show that these calculations yield satisfactory results when compared with measured data. Finally, in Section 6 we discuss the use of the measured or calculated enthalpy vs. composition diagram as a good approximation to the free energy diagram to predict the homogeneity range of the amorphous phase under different kinetic constraints.

2. Experimental data

A mechanical alloying technique, namely, ball milling of mixed elemental powders, has been employed to form amorphous $Zr_{1-x}Al_x$ alloys. A full description of experimental details can be found in our previous publications [17, 18]. Elemental Zr and Al powders were mixed and sealed in Ar, and then ball-milled for 24 h. The product phases were identified using X-ray diffraction in step-scanning mode. Cu $K\alpha$ X-rays were generated by a rotating anode operating at 7.5 kW, and filtered by a diffracted-beam graphite monochromator. Transmission electron microscopy (TEM) was

performed using a JEOL-2000FX microscope operating at 200 kV. TEM samples were prepared by pressing powder into disks, which were subsequently mechanically thinned and ion-milled at liquid nitrogen temperature until electron transparent. Impurity incorporation from milling tools was found to be insignificant (less than 1 at.%).

For $0 < x \leqslant 0.15$, the ball milling yielded h.c.p. solid solutions, and for $0.175 \leqslant x \leqslant 0.40$, an amorphous phase. These results are in agreement with a previous report on the same system [19]. Figure 1 shows an X-ray diffraction pattern for $Zr_{60}Al_{40}$ powder after 24 h ball milling. Broad peaks characteristic of an amorphous structure are observed without indication of presence of crystalline phases. A TEM bright-field image together with a corresponding selected-area diffraction pattern is shown for the $Zr_{80}Al_{20}$ powder in Fig. 2. Lack of crystalline contrast in both bright- and dark-field micrographs and halos in the diffraction pattern confirm the amorphous structure. When heating the powder in a DSC-7 power-compensated differential scanning calorimeter, well-defined exothermic peaks, corresponding to the crystallization of these amorphous alloys, were observed. The enthalpies of transformation to equilibrium for the amorphous alloys as well as for h.c.p. solid solutions were measured by integrating these relatively narrow peaks. For details of the results, the readers are referred to refs. 17 and 18. We have not studied alloys with $x > 0.40$ for several reasons. First, a metastable crystalline phase has been reported to form by ball milling at $x = 0.50$ [19]. Second, for $x > 0.50$, the milling efficiency is very low due to a large amount of ductile Al [19]. Moreover, as will be discussed later, for $x \leqslant 0.40$, all equilibrium compounds almost fall on the same common tangent line in an enthalpy of formation vs. composition diagram. The measured enthalpy of crystallization is thus nearly independent of relative
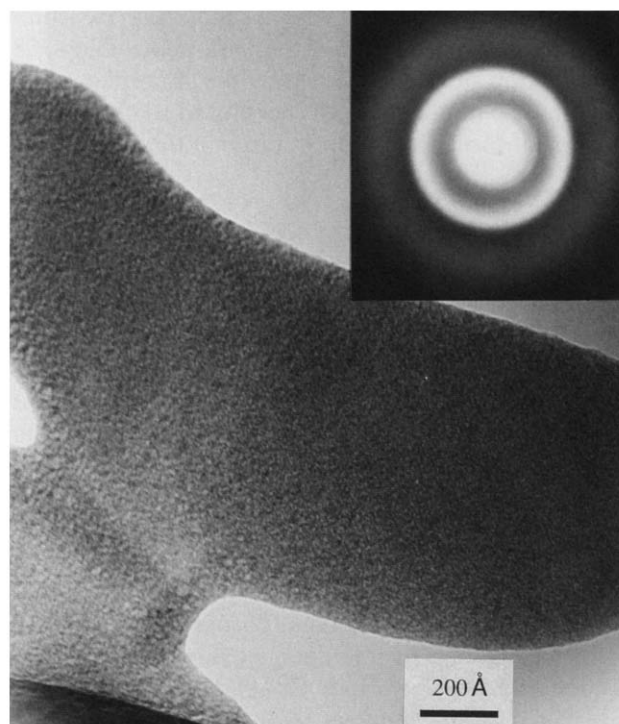

Fig. 2. Bright-field TEM image and corresponding selected-area diffraction pattern for 24 h ball-milled $Zr_{80}Al_{20}$ powder, showing an amorphous structure.

amounts of equilibrium phases in the crystallization product. This reduces errors associated with the possible presence of more than two equilibrium phases, reflected in the X-ray diffraction pattern of the crystallization product for $x \geqslant 0.25$. For the equilibrium compounds, the enthalpies of formation were obtained from ref. 5.

Amorphous Zr–Ni alloys can be formed by a number of techniques such as rapid quenching [6(a), 20, 21], co-deposition [22(a), 22(b)], solid-state interdiffusion reactions [1, 23–25], and mechanical alloying [4]. Crystallization enthalpies we cite in this paper were obtained from ref. 6(a) for amorphous alloys formed by melt-quenching. Later, Altounian et al. [20] and McKamey et al. [21] reported enthalpy of crystallization data of the same magnitude for Ni-rich alloys, but slightly (by about 1–2 kJ mol^{-1}) smaller on the Zr-rich side. The final crystallization products have been confirmed to be the equilibrium compounds [20]. The enthalpy of formation of an amorphous $Ni_{68}Zr_{32}$ alloy from elemental Zr and Ni by solid-state interdiffusion reaction in multilayer composite films has been measured directly by Cotts et al. [24(a)], Highmore et al. [24(b)] and Eckert et al. [25]. These reports agree with each other to give $\Delta H_{f, am} = -35 \pm 5$ kJ mol^{-1}. The enthalpies of formation of the equilibrium compounds have been measured by Henaff et al. [6(a)] and Gachon et al. [6(b)].
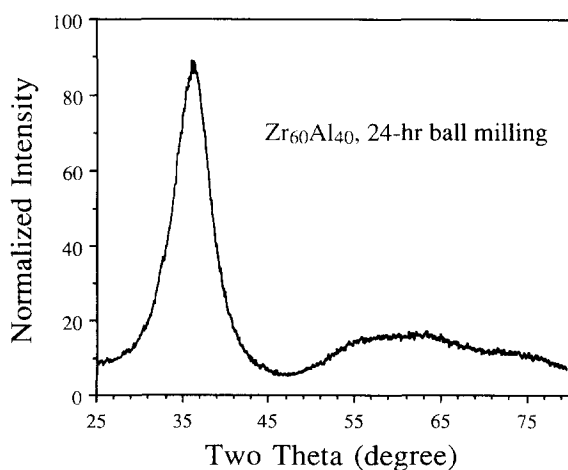

Fig. 1. X-ray diffraction pattern (Cu Kα radiation) for 24 h ball-milled $Zr_{60}Al_{40}$ powder, showing an amorphous structure.

For both Zr–Al and Zr–Ni systems, the measured enthalpy of crystallization of the amorphous alloys, *i.e.* the enthalpy difference between the amorphous and crystallized phase, ΔH_{1-c}, has been used to obtain their enthalpy of formation, $\Delta H_{f,\,am}$, through the relationship

$$\Delta H_{f,\,am} = \Delta H_{f,\,c} - \Delta H_{1-c} \tag{1}$$

where $\Delta H_{f,\,c}$ is the enthalpy of formation of the equilibrium phases. The errors of these experimental enthalpies of formation of the amorphous phase are small compared with the relatively large magnitude of the enthalpy of formation itself. In fact, in the enthalpy of formation figures shown in the following sections, error bars of these data points are often smaller than the data point symbols.

3. CALPHAD calculations

The CALPHAD equations and parameters needed for the calculation of free energy or enthalpy *vs.* composition curves for various Zr–Al and Zr–Ni phases were taken from Saunders [26(a)] and Saunders and Miodownik [2] respectively. An enthalpy of formation *vs.* composition diagram for the Zr–Ni system has in fact already been constructed in ref. 2. Since the free energy has not been measured to compare with calculations, only the enthalpy of formation (ΔH_f) diagrams will be discussed in Sections 3–5. As will be discussed later in Section 6, the ΔH_f diagram is expected to adequately approximate the free energy diagram at low temperatures. In Figs. 3 and 4, ΔH_f *vs.* composition curves calculated using CALPHAD data, as well as curves calculated based on procedures discussed in the following sections, are shown for Zr–Al at 450 K and Zr–Ni at 500 K, respectively. These temperatures are chosen because they are typical values encountered in solid-state amorphization reactions [1, 2, 17]. The experimental data, discussed in Section 2, are included for comparison. The Zr concentration, $(1-x)$, is used for the horizontal axis in Fig. 4 to keep the original format used by Saunders and Miodownik [2], which has been widely cited by other authors [1, 22].

In the diagram for Zr–Al, Fig. 3, a solid line, labeled "equilibrium", is drawn to represent the equilibrium common tangent between the h.c.p. solid solution and the first observed compound, Zr_2Al. As mentioned above, all compounds with less than 40 at.% Al lie nearly on the same line. This reduces possible errors in calorimetric measurements due to the presence of multiple equilibrium phases in the final crystallization product. For Zr–Al, it is seen that for the h.c.p. solid solution the calculated curve agrees with the experimental data reasonably well, both indicating a negative enthalpy of formation of the solution phase. However
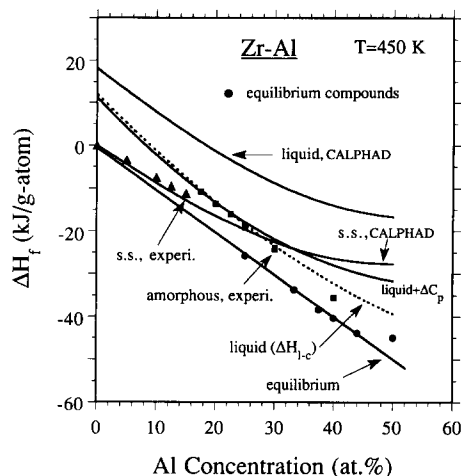

Fig. 3. Enthalpy of formation *vs.* composition for the Zr–Al system. Calculations for h.c.p. solid solution and undercooled liquid are based on data from Saunders [26(a)]. The enthalpies of formation for compounds, labeled with circles, were obtained from ref. 5. The "equilibrium" line represents the common tangent between the Zr-rich terminal solid solution and equilibrium compound, Zr_2Al. The experimental data for the h.c.p. solid solution (triangles) and the amorphous phase (squares) are included for comparison [17]. The modified liquid curve is calculated by incorporating the ΔC_p contribution to $\Delta H_{f,\,am}$ obtained from eqn. (13). The curve based on ΔH_{1-c} (dashed line) is calculated using eqns. (1) and (5), with ΔH calculated using eqn. (13) (see Section 5).
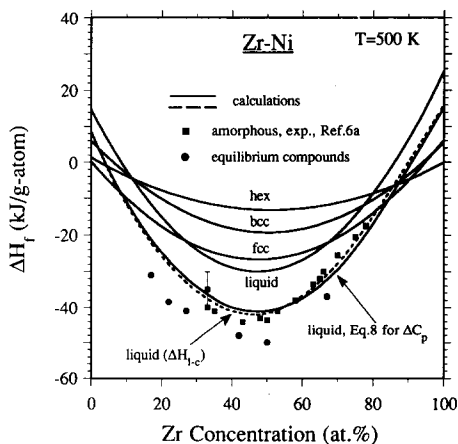

Fig. 4. Enthalpy of formation *vs.* composition for the Zr–Ni system. The Zr concentration $(1-x)$ is used for the horizontal axis following Saunders and Miodownik [2]. Calculations for solid solutions and liquid are from ref. 2. The enthalpies of formation for compounds (circles) are from refs. 6(a) and 6(b). The experimental data for the amorphous phase (squares) are included for comparison [6(a)]. The datum point with error bar was obtained from Cotts *et al.* for amorphization of multilayered films in a calorimeter [24]. The modified liquid curve was obtained after incorporating the ΔC_p contribution to $\Delta H_{f,\,am}$, as obtained from eqn. (14). The curve based on ΔH_{1-c} (dashed line) was calculated using eqns. (1) and (5), with ΔH calculated using eqn. (14) (see Section 5).

the calculated curve for the undercooled liquid (top curve in Fig. 3), which we use to represent the amorphous phase, shows poor agreement with the experimental data. In fact, the curve of the undercooled liquid lies above that of the h.c.p. solid solution, thus predicting no amorphization.

As shown in Fig. 4, an amorphous phase, metastable with respect to the intermetallic compounds, is predicted by the CALPHAD method in the Zr–Ni system. This is evidenced by the fact that the calculated $\Delta H_{f,\,am}$ curve (the curved labeled "liquid" in Fig. 4) lies below those of solid solutions over the central range of compositions. However, the undercooled liquid curve does not match the experimental data quantitatively [2]. Therefore, the straightforward extrapolation of the CALPHAD method does not lead to satisfactory results for the amorphous phase in either Zr–Al or Zr–Ni systems. Although such an extrapolation sometimes adequately demonstrates that the undercooled liquid possesses a large negative enthalpy of formation, the stability of the amorphous phase is frequently underestimated. A significant difference between the enthalpy calculated for the liquid phase and that measured for the amorphous phase is not a rare phenomenon. This difference is termed H^{L-A} by Saunders, who has compiled data for some 10 systems and found that H^{L-A} is generally about 10–20 kJ mol^{-1} for binary metallic alloys [27]. As discussed in the Introduction, a major source of this discrepancy is the invalidity of extrapolation to a large degree of undercooling. As the temperature decreases, the liquid goes through significant changes in entropy. This is reflected in its specific heat, which increases as the temperature decreases, followed by a sharp decrease at the glass transition temperature to a value close to that of the solid. These effects have to be accounted for when using the undercooled liquid to represent the amorphous phase [10, 28–30], as discussed in the next section.

4. Effects of the excess specific heat

As mentioned above, the increasing degree of order in the liquid upon continuous undercooling gives rise to an increasing excess specific heat in the liquid, ΔC_p. At some temperature, T_s, the entropy of the liquid will become equal to that of the crystalline solid. It has been suggested that the specific heat of the liquid will drop sharply at a temperature near but higher than T_s and become very similar to that of the crystalline phases [10, 28–30]. T_s is the ideal glass transition temperature, i.e. the lower limit of the glass transition temperature observed in practice. Using the isentropic condition at T_s [11–16, 31], we obtain for temperatures $T \leqslant T_s$,

$$\Delta S_{1-c}(T) = \Delta S_m - \int_{T_s}^{T_m} \Delta C_p \, \mathrm{d} \ln T = 0 \qquad (2)$$

where T_m is the melting temperature, ΔS_{1-c}, the entropy difference between the liquid and the crystallized phases, and ΔS_m, the entropy of fusion. This gives

$$\int_{T_s}^{T_m} \Delta C_p \, \mathrm{d} \ln T = \Delta S_m \qquad (3)$$

Accompanying the entropy loss, the enthalpy loss due to ΔC_p during undercooling to temperature T is given by

$$\Delta H(T) = \int_{T}^{T_m} \Delta C_p \, \mathrm{d}T \qquad (4)$$

Similar to eqn. (2) the enthalpy difference between the liquid and crystalline states at temperature $T < T_m$ is [11–16]:

$$\Delta H_{1-c}(T) = \Delta H_m - \int_{T}^{T_m} \Delta C_p \, \mathrm{d}T = \Delta H_m - \Delta H(T) \qquad (5)$$

where ΔH_m is the enthalpy of fusion. In the following treatment, the thermodynamic functions will not be written as explicit functions of T, because they are calculated for fixed $T < T_s$.

When ΔC_p is known, the desired quantities, ΔH and ΔH_{1-c}, can be calculated using eqns. (4) and (5). However, little experimental data for the heat capacity of the supercooled liquid is available, let alone its temperature dependence through the entire undercooled regime and its composition dependence for a binary alloy. Therefore, some approximating assumptions need to be made. A typical expression used for a polynomial fit for the temperature dependence of heat capacity gives, neglecting higher order terms [32–34],

$$\Delta C_p = AT + B + CT^{-2} + \ldots \qquad (6)$$

where A, B, and C are temperature-independent constants. In the following, we will consider two contrasting cases often assumed by other authors. One is the simplest approximation of a temperature-independent ΔC_p [11–16], i.e.

$$\Delta C_p = B \qquad (7)$$

and the other is a hyperbolic rapid increase of ΔC_p upon undercooling [29, 30], namely,

$$\Delta C_p = C/T^2 \qquad (8)$$

where B and C are composition-dependent coefficients. For eqns. (7) and (8), the temperature T is in the interval $T_s < T < T_m$. Using the isentropic condition, eqn. (3), we have

$$B = \Delta S_m / \ln(T_m/T_s) \qquad (9)$$

and

$$C = 2\Delta S_m / (T_s^{-2} - T_m^{-2}) \qquad (10)$$

Owing to the nearly symmetric shape of the heat of mixing as a function of composition, and that ΔC_p is relatively small for pure elements [34, 35], some authors have assumed a parabolic composition dependence of ΔC_p with the maximum at $x = 50$ [30, 36], such that for the two assumed temperature dependences,

$$B = B'x(1-x) \qquad (11)$$

or

$$C = C'x(1-x) \qquad (12)$$

where B' and C' are constants. In our calculations, we use eqns. (9) and (10) to calculate ΔC_p directly for all compositions, without assuming a particular functional form for the composition dependence of ΔC_p. A comparison will be made at the end of this section with the parabolic functions assumed in eqns. (11) and (12).

According to eqn. (4), for undercooling to below the glass transition temperature, the enthalpy loss of the undercooled liquid associated with ΔC_p is

$$\Delta H = B(T_m - T_s) = \Delta S_m(T_m - T_s)/\ln(T_m/T_s) \qquad (13)$$

for ΔC_p following eqn. (7), and

$$\Delta H = C(1/T_s - 1/T_m)$$
$$= 2\Delta S_m(T_s^{-1} - T_m^{-1})/(T_s^{-2} - T_m^{-2}) \qquad (14)$$

for ΔC_p following eqn. (8). To calculate ΔH using eqns. (13) and (14) one needs data for T_m, T_s, and ΔS_m. The melting temperature T_m can be estimated for all compositions from the solidus lines in the corresponding equilibrium phase diagram. The experimental glass transition temperature, T_g, is used in the following calculations to approximate T_s, assuming that the liquid loses most of its entropy of fusion when undercooled to T_g. This is based on the assumption that ΔC_p drops precipitously around T_g such that the entropy loss between T_g and T_s is small compared with that in the rather wide temperature interval between T_m and T_g. The possibility that a portion of ΔS_m is retained at T_g will be discussed in Section 6. In the following treatment, we will assume $\Delta S(T_g) = 0$ for simplicity. For pure elements, ΔS_m can be found in the literature. Richard's rule [37], which states that the heat of fusion is proportional to the melting temperature with a nearly

constant proportionality factor for all elements, can be extended to equiatomic compounds. The proportionality factor, i.e. entropy of fusion, has been observed to be approximately 12.5 J K^{-1} mol^{-1} [37, 38]. A linear interpolation between the element and the equiatomic compound is used in our calculations to obtain ΔS_m of all other compositions. For most easy glass-forming systems, $T_g \approx 0.5\ T_m$ [28]. For such a value of T_g, eqns. (13) and (14) would give values of ΔH to within a few percent of each other for large undercooling to T below T_g, $0.7\ \Delta H_m$ (eqn. (13)) vs. $0.667\ \Delta H_m$ (eqn. (14)). For relatively poor glass formers with $T_g \approx 0.3\ T_m$, the difference between eqns. (13) and (14) will increase to about 15%. In our calculations, we will use both equations and compare the results.

If T_s values are known for all compositions, x, then ΔC_p can be determined from eqns. (7)–(10), and the calculations of ΔH can be carried out using eqns. (13) and (14). For amorphous Zr–Ni alloys, T_g has been measured over a wide range of compositions [22(a), 39], and for amorphous Zr–Al alloys, the crystallization temperature T_x, which is likely to be within 50 K of T_g [39, 40], has been obtained from our calorimetry experiments at a heating rate of 5 K min^{-1}. These T_g and T_x values are used in our calculations to approximate T_s. No data of T_g for the pure metals involved are available. It has been calculated that T_g is likely to be in the range of 0.25–0.3 T_m [10, 34], where T_m is the melting point of the metal. We thus chose to extrapolate linearly the known T_g (or T_x) to pure metals and assume that the extrapolation is reasonable when the extrapolated value falls in the above range.

The calculations described above yield a set of discrete points which serve to construct an interpolated curve describing the contribution of ΔC_p to the enthalpy of formation of the undercooled liquid. In Fig. 3 for the Zr–Al system and Fig. 4 for the Zr–Ni system, this contribution ΔH, calculated using eqns. (13) and (14), respectively, has been added to the directly extrapolated CALPHAD curves described in Section 3, to give the modified liquid curves. For each system, we have only shown one curve calculated using either eqn. (13) or eqn. (14), since different choices of ΔC_p (eqns. (7) or (8)) give very similar results to within a few percent to approximately 15%. In the case of Zr–Ni, an impressive improvement in matching the experimental data has been achieved. This demonstrates that the incorporation of ΔC_p effects is necessary and that the procedures and assumptions we followed above are reasonable. In the case of Zr–Al, the modified undercooled liquid curve also agrees well with the experimental data, except for near the equiatomic composition. Clues for the origin of this latter error can be found in the equilibrium Zr–Al phase diagram, where all liquidus lines are dashed, indicating tentative

characterization [41]. In fact, calculation using earlier parameters for the liquid phase polynomial [26(b)], which were obtained with even less experimental input, gives an obviously erroneous undercooled liquid curve that deviates considerably from experimental data for all compositions [18], with or without the ΔC_p correction term. (There are also two sets of parameters for the h.c.p. solution [26(b)], which yield somewhat different calculated curves that are both close to experimental data for $x < 15$, and the difference is not significant enough to change any conclusions in this paper.) In contrast, in the absence of such a drawback of insufficient input for determining parameters, the amorphous Zr–Ni curve closely matches the experimental data. For Zr–Al, the next section will demonstrate that the calculation of the enthalpy of formation based on the enthalpy of crystallization can yield better agreement with experimental data.

We finally note that in systems for which data for T_g or T_x data are very limited, the simple parabolic composition dependence of ΔC_p assumed by some authors [30, 36] (eqns. (11) and (12)) may be used to estimate ΔC_p for all compositions, with the constants B' and C' determined by eqns. (11) and (12), using available data sets $(T_m, T_s, \Delta S_m)$. For Zr–Ni and Zr–Al, it turns out that this approach yields similar results for x in the central composition range. In fact, T_s values calculated using eqns. (9) and (10) with these estimated ΔC_p compare favorably with experimental T_g, especially when eqn. (8) is used. The parabolic composition dependence, however, is only an over-simplified assumption. It will yield a vanishing ΔH for $x = 0$ and $x = 1$. It should be pointed out that, although ΔC_p is smaller for pure metals than for alloys [34, 35], the integration over the undercooled regime to T_g would still constitute a substantial, certainly non-zero, contribution to the thermodynamic functions. This fact has been taken into account in our calculations by using eqns. (9) and (10) and estimated T_g for pure metals, but the estimated ΔH is likely to contain more error than for alloys with known T_g or T_x.

5. Enthalpy of crystallization

The difference in enthalpy between the undercooled liquid and the crystallized phases, or enthalpy of crystallization, ΔH_{1-c}, can be easily computed using eqn. (5), where $\Delta H_m = \Delta S_m T_m$, and ΔH is obtained from eqns. (13) or (14). The calculated data are shown in Figs. 5 and 6 together with experimental data for Zr–Al and Zr–Ni, respectively. It can be seen that the use of eqn. (8) for ΔC_p gives a slightly higher ΔH_{1-c} than using eqn. (7). This difference between different choices of ΔC_p, which was small when calculating ΔH in Figs.
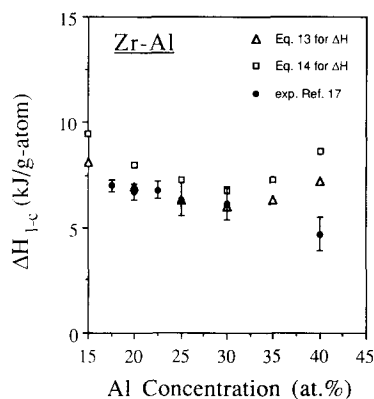

Fig. 5. Calculated and measured enthalpy of crystallization vs. Al concentration for the $Zr_{1-x}Al_x$ amorphous alloys. Calculations are based on eqn. (5), with ΔH calculated using eqn. (13) (triangles) or eqn. (14) (squares). Filled circles with error bar represent experimental data.
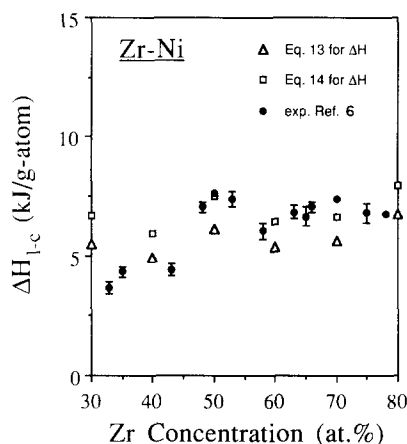

Fig. 6. Calculated and measured enthalpy of crystallization vs. Zr concentration for the $Zr_{1-x}Ni_x$ amorphous alloys. Calculations are based on eqn. (5), with ΔH calculated using eqn. (13) (triangles) or eqn. (14) (squares). Filled circles with error bar represent experimental data.

3 and 4, is now noticeable because the magnitude of ΔH_{1-c} is smaller than that of ΔH. Nevertheless, considering all the approximations and possible errors, we consider both calculated data sets to agree well with experimental data. Using these data, the enthalpy of formation of the amorphous phase, $\Delta H_{f,am}$, has been calculated using eqn. (1). The resulting curves have also been included in Figs. 3 and 4, which have significantly wider vertical scales than Figs. 5 and 6. In the Zr–Ni case, a remarkable agreement is observed between the $\Delta H_{f,am}$ curve calculated from the modified CALPHAD method (Section 4, incorporating eqn. (14)) and that from eqns. (1) and (5). This reflects the reliability of the procedures described in this paper. In the Zr–Al case, $\Delta H_{f,am}$ calculated from eqns. (1) and (5) agrees with experiment better than the modified CALPHAD curve (Section 4). A possible source of error for the latter has been discussed in Section 4.

6. The homogeneity range of the amorphous phase

Assuming metastable thermodynamics to govern phase formation, the accurate determination of the homogeneity range of the amorphous phase in a binary system requires a diagram of the free energy of formation, ΔG_f, vs. composition. Although the entropic term is expected to be only a fraction of the larger enthalpic term for low temperatures commonly used for amorphous phase synthesis, a moderate difference may exist between the enthalpy and the free energy, when both are calculated using the CALPHAD method [2]. The magnitude of this difference can be estimated by inspecting the available measured or calculated data in the literature for binary systems. For crystalline compounds, the contribution of the entropic term to the free energy of formation is typically on the order of < 1–2 kJ mol^{-1} at temperatures below 500 K. For solid solutions, the entropic contribution is on the order of a few kJ mol^{-1} for these low temperatures (to be compared with that for ideal solutions, less than 3 kJ mol^{-1}). CALPHAD calculations described in this paper indicate an entropic contribution of less than 3 kJ mol^{-1} for h.c.p. and f.c.c. Zr–Ni solid solutions [2], and only less than 1 kJ mol^{-1} for the Zr–Al h.c.p. solid solution [26(a)] (a larger value of less than 6 kJ mol^{-1} was obtained using earlier parameters for the CALPHAD polynomial [26(b)]). Due to a larger entropy term for the liquid in the CALPHAD extrapolations, a larger entropic contribution to the formation free energy of the undercooled liquid is usually observed, e.g. 7 kJ mol^{-1} for the Zr–Ni system [2] and 4 kJ mol^{-1} for the Zr–Al system [26(a)]. Adding the entropy terms to yield free energy of formation curves will change the relative positions of the enthalpy curves to some extent. Since the curves often shift to the same direction, i.e. become more negative, to a comparable degree, the qualitative and even some quantitative features (e.g. cross-over and common tangent compositions) in the free energy diagram are often approximately preserved in the enthalpy diagram.

Moreover, we note that the incorporation of a ΔC_p correction to the CALPHAD calculations discussed in Sections 4 and 5 would significantly reduce the difference between the calculated ΔH_f and ΔG_f curves for the amorphous (liquid) phase. This is because the ΔC_p term takes into account a continuous decrease of the entropy of the liquid during undercooling, $\Delta S(T)$, according to

$$\Delta S(T) = \int_T^{T_m} \Delta C_p \, d \ln T \qquad (15)$$

For temperatures below T_g, we have assumed that the undercooled liquid is nearly isentropic with the crys-

tallized phases. Hence the free energy difference between the liquid and the crystallized material is

$$\Delta G_{l-c} = \Delta H_{l-c} \qquad (16)$$

Similar to eqn. (1), the free energy of formation of the undercooled liquid is

$$\Delta G_{f, \, am} = \Delta G_{f, \, c} - \Delta G_{l-c} \qquad (17)$$

where $\Delta G_{f, c}$ is the formation free energy of the equilibrium crystalline phases which are usually ordered compounds having a small entropy of formation [2, 26(b)]. The $\Delta G_{f, am}$ curve obtained from eqns. (16) and (17) would thus be quite close to the $\Delta H_{f, am}$ curve obtained from eqn. (1). As an example, we show in Fig. 7 the calculated $\Delta H_{f, am}$ (Section 5) and $\Delta G_{f, am}$ (eqns. (16) and (17)) curves for the Zr–Al undercooled liquid. They almost overlap for a wide range of compositions. If it is assumed that there is still a remaining entropy difference between the undercooled liquid and the crystalline phases at low temperatures, e.g. on the order of 0.25 ΔS_m, eqn. (16) would not be valid, and the $\Delta H_{f, am}$ and $\Delta G_{f, am}$ curves would shift apart from each other. Nonetheless, the difference between these two curves is likely to be small. Also shown in Fig. 7 are the ΔH_f and ΔG_f curves for the Zr–Al h.c.p. solid solution calculated based on CALPHAD data of ref. 26(a). It can be seen that these two curves are also very close to each other (some minor difference existed in the calculations using an earlier set of parameters for the CALPHAD polynomial [26(b)]). For comparison, the experimental enthalpy data are also included.
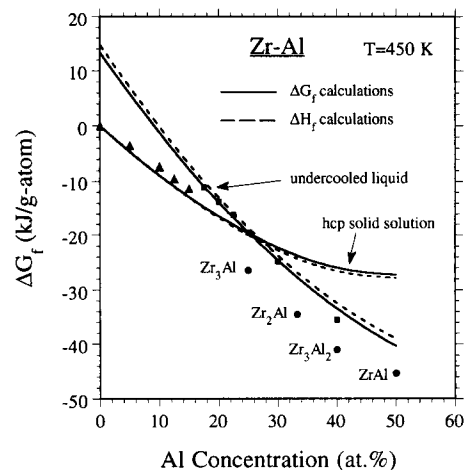

Fig. 7. Comparison of the enthalpy of formation and the free energy of formation curves calculated for the Zr–Al system (see text). The curves for the amorphous phase (liquid) are calculated using our approach outlined in Section 5. The formation free energy data for the compounds (circles) were obtained from ref. 26(b). Experimental enthalpy data from ref. 17 (same as Figs. 3 and 5) are included for comparison. The curves for the h.c.p. solid solution are calculated based on ref. 26(a).

From the ΔG_f curves and ΔH_f curves in Fig. 7 for the Zr–Al system, the crossover of the h.c.p. solid solution curve and the liquid curve is close to $x^* = 0.25$. This is the minimum solute concentration needed for the amorphous phase to be more stable than the h.c.p. solid solution assuming the system to be constrained to a single phase. Such polymorphous constraints are possible for alloys formed by vapor deposition [42], ion irradiation [43], and mechanical alloying [17]. The curve fits to the experimental enthalpy data would give $x^* = 0.22$ [17]. Even when less accurate CALPHAD parameters are used for the ΔH_f and ΔG_f calculations for the h.c.p. solid solution [26(b)], the predicted crossover also occurs in the range of $x^* = 0.20$–0.25 [44]. The spread in these values is small and comparable with the experimental composition interval used in ref. 17, $\Delta x = 0.025$. During ball milling, this critical concentration was shifted to $x^* = 0.175$ due to the energy stored in the cold-worked material [17]. If the system is not constrained to a single phase and a metastable equilibrium, determined by a common tangent construction, is present, the minimum x required for an amorphous single phase would be approximately $x = 0.35$–0.40. Again, ΔG_f, ΔH_f, and experimental curves give similar results. From these comparisons and the discussions in preceding paragraphs, we suggest that it is adequate to use enthalpy curves to estimate the homogeneity range for the amorphous phase at low temperatures. The advantage of this approach is that experimental measurement of the enthalpy change is relatively straightforward.

Similarly, for Zr–Ni, the ΔG_f and ΔH_f curves calculated based on our approach outlined in this paper do not differ much. In Fig. 4 for Zr–Ni, the homogeneity range of the amorphous phase predicted by polymorphous constraints is approximately $0.15 < x < 0.90$ (note that the horizontal axis is in $1 - x$). This is in very good agreement with experimental values determined by codeposition, $0.2 < x < 0.9$, when polymorphous constraints are likely to exist [22(a), 22(b)]. The common tangents in Fig. 4, on the other hand, predict a homogeneity range of approximately $0.35 < x < 0.80$ for the amorphous phase. Previous measurements of interfacial compositions in standard diffusion couples give a range of $0.45 < x < 0.68$ [25, 45, 46], which is somewhat narrower than the prediction. Recent direct measurements of the common tangent compositions in the Hf–Ni system indicated a broader homogeneity range of the amorphous phase than that determined in standard elemental diffusion couples [47]. This finding suggests that a standard diffusion couple experiment may not be suitable for the determination of the equilibrium compositions, due to lack of equilibrium or non-linear composition profiles. It may also explain our observation for the Zr–Ni system that the calculated homogeneity range of the amorphous phase is wider than that measured by previous authors.

7. Conclusions

(i) We have confirmed that a straightforward extrapolation of the thermodynamic functions for the liquid employed in the CALPHAD method is insufficient to describe the thermodynamic functions of the amorphous phase in the Zr–Al and Zr–Ni systems. The stability of the amorphous phase is usually underestimated when such extrapolation is used, typically by 10–20 kJ mol^{-1}.

(ii) The incorporation of the excess specific heat of the undercooled liquid considerably improves the agreement with experimental data, especially for Zr–Ni. The result is relatively insensitive to the choice of the functional form of ΔC_p for large undercooling to below T_g.

(iii) The CALPHAD thermodynamic functions, including correction terms, may be inadequate if there is large uncertainty in the experimental input, as shown for the undercooled Zr–Al liquid. The use of recent parameters derived with more experimental input yielded improvement over earlier results.

(iv) The enthalpy of crystallization is on the order of a few kilojoules per mole for amorphous Zr–Al and Zr–Ni alloys, as well as for many other binary amorphous alloys. Calculations using assumed ΔC_p functions yield enthalpy of crystallization values in close agreement with experimental data. These calculations, combined with experimental data for equilibrium compounds, provide an alternative determination of the enthalpy of formation. The agreement with experimental data is satisfactory for both Zr–Al and Zr–Ni systems.

(v) It should be pointed out that the approach described in this paper involves many assumptions. The aim of this paper is to improve the CALPHAD extrapolations using simple procedures. A comprehensive, rigorous treatment of the problem must await the establishment of an experimental data base and progress in understanding of liquid behavior during undercooling.

(vi) We have shown that the ΔH_f and ΔG_f diagrams calculated using our approach do not differ much from each other at low temperatures, and the metastable equilibria determined from these diagrams are in close agreement with those found in the experiments. It is therefore adequate to use measured enthalpy curves as an approximation to the free energy curves to predict the metastability of phases.

Acknowledgments

References

1 W. L. Johnson, *Prog. Mater. Res., 30* (1986) 81.

2 N. Saunders and A. P. Miodownik, *J. Mater. Res., 1* (1986) 38.

3 A. R. Miedema, *Philips Tech. Rev., 36* (1976) 217.
F. R. de Boer, R. Boom, W. C. M. Mattens, A. R. Miedema and A. K. Niessen, in F. R. de Boer and D. Pettifor (eds.), *Cohesion in Metals*, Elsevier, North Holland, Amsterdam, 1988.

4 A. W. Weeber and H. Bakker, *Physica B, 153* (1988) 93.

5 R. J. Kematick and H. F. Franzen, *J. Solid State Chem., 54* (1984) 226.

6 (a) M. P. Henaff, C. Colinet, A. Pasturel and K. H. J. Buschow, *J. Appl. Phys., 56* (1984) 307.
(b) J. C. Gachon, M. Dirand and J. Hertz, *J. Less-Common Met., 92* (1983) 307.

7 A. W. Weeber, *J. Phys. F, 17* (1987) 809.

8 L. Kaufman and H. Bernstein, *Computer Calculations of Phase Diagrams*, Academic Press, New York, 1970.
J. L. Murray, *Bull. Alloy Phase Diagr., 4* (1983) 81.
N. Saunders, *CALPHAD, 9* (1985) 297.

9 R. B. Schwarz, P. Nash and D. Turnbull, *J. Mater. Res., 2* (1987) 456.

10 (a) H. S. Chen and D. Turnbull, *J. Chem. Phys., 48* (1968) 2560.
(b) L. Battezzati, *Phil. Mag. B, 61* (1990) 511.

11 D. Turnbull, *J. Appl. Phys., 21* (1950) 1022.

12 J. D. Hoffman, *J. Chem. Phys., 29* (1958) 1192.

13 D. R. H. Jones and G. A. Chadwick, *Phil. Mag., 24* (1971) 995.

14 C. V. Thompson and F. Spaepen, *Acta Metall., 27* (1979) 1855.

15 L. Battezzati and E. Garrone, *Z. Metallkd., 75* (1984) 305.

16 K. S. Dubey and P. Pamachandrarao, *Acta Metall., 32* (1983) 91.

17 E. Ma and M. Atzmon, *Phys. Rev. Lett., 67* (1991) 1126.

18 E. Ma and M. Atzmon, *Mater. Sci. Forum, 88-90* (1992) 467.

19 H. J. Fecht, G. Han, Z. Fu and W. L. Johnson, *J. Appl. Phys., 67* (1990) 1744.

20 Z. Altounian, Guo-hua Tu and J. O. Strom-Olsen, *J. Appl. Phys., 54* (1983) 3111.

21 C. G. McKamey, D. M. Kroeger, D. S. Easton and J. O. Scarbrough, *J. Mater. Sci., 21* (1986) 3863.

22 (a) T. Minemura, J. J. van den Broek and J. L. C. Daams, *J. Appl. Phys., 64* (1988) 4770.
(b) J. B. Rubin and R. B. Schwarz, *Mat. Res. Soc. Symp. Proc., 230*, in press.

23 B. M. Clemens, R. B. Schwarz and W. L. Johnson, *J. Non-Cryst. Solids, 61/62* (1984) 817.

24 (a) E. J. Cotts, W. J. Meng and W. L. Johnson, *Phys. Rev. Lett., 57* (1986) 2296.
(b) R. J. Highmore, J. E. Evetts, A. L. Greer and R. E. Somekh, *Appl. Phys. Lett., 50* (1987) 566.

25 J. Eckert, L. Schultz and K. Urban, *J. Mater. Res., 6* (1991) 1874.

26 (a) N. Saunders, *Z. Metallkd., 80* (H.12) (1989) 895.
(b) N. Saunders and V. G. Rivlin, *Mater. Sci. Technol., 2* (1986) 521.

27 N. Saunders, *Inter. J. Rapid Solidification, 1* (1984-85) 327.

28 M. T. Clavaguera-Mora and N. Clavaguera, *J. Mater. Res., 4* (1989) 906.

29 F. Gartner and R. Bormann, *Colloq. Phys., 51* (1990) C4-95.
R. Bormann, F. Gartner and K. Zoeltzer, *J. Less-Common Met., 145* (1988) 19.

30 G. Cocco, I. Soletta, L. Battezzati, M. Baricco and S. Enzo, *Phil. Mag. B, 61* (1990) 473.

31 W. Kauzmann, *Chem. Rev., 42* (1948) 219.

32 *JANAF Thermodynamical Tables*, 3rd edition, *J. Phys. Chem. Ref. Data, 14*, suppl. 1 (1985).

33 I. Barin, O. Knacke and O. Kubaschewski, *Thermodynamical Properties of Inorganic Substances*, Supplement, Springer, Berlin, 1977.

34 H. J. Fecht, *Mater. Sci. Eng. A, 133* (1991) 443.

35 J. H. Perepezko and J. S. Paik, *J. Non-Cryst. Solids, 61/62* (1984) 113.

36 R. J. Highmore and A. L. Greer, *Nature, 339* (1989) 363.

37 R. A. Swalin, *Thermodynamics of Solids*, Wiley, New York, 1962, p. 60.

38 D. Goodman, J. W. Cahn and L. H. Bennett, *Bull. Alloy Phase Diagr., 2* (1973) 29.

39 K. H. J. Buschow, *J. Phys. F, 14* (1984) 593.

40 L. Battezzati and A. L. Greer, *J. Mater. Res., 3* (1988) 570.

41 T. B. Massalski (ed.), *Binary Alloy Phase Diagrams*, Vol. 1, ASM, Metals Park, OH, 1986, p. 187.

42 N. Saunders and P. Miodownik, *J. Mater. Sci., 22* (1987) 629.

43 W. L. Johnson, Y.-T. Cheng, M. van Rossum and M.-A. Nicolet, *Nucl. Instrum. Methods, Phys. Res. B, 7/8* (1985) 657.

44 E. Ma and M. Atzmon, *Mod. Phys. Lett. B, 6* (1992) 127.

45 J. C. Barbour, *Phys. Rev. Lett., 55* (1985) 2872.

46 G. C. Wong, W. L. Johnson and E. J. Cotts, *J. Mater. Res., 5* (1990) 488.

47 W. S. L. Boyer and M. Atzmon, in M. O. Thompson, M. Aziz and G. B. Stephenson (eds.), *Kinetics of Phase Transformations*, MRS, Pittsburgh, 1991, p. 189.